

# DMamba: Decomposition-enhanced Mamba for Time Series Forecasting

Ruxuan Chen\*

rc1c24@soton.ac.uk

Harbin Engineering University  
Harbin, China

Fang Sun\*†

fsun@cnu.edu.cn

Capital Normal University  
Beijing, China

## Abstract

State Space Models (SSMs), particularly Mamba, have shown potential in long-term time series forecasting. However, existing Mamba-based architectures often struggle with datasets characterized by non-stationary patterns. A key observation from time series theory is that the statistical nature of inter-variable relationships differs fundamentally between the trend and seasonal components of a decomposed series. Trend relationships are often driven by a few common stochastic factors or long-run equilibria, suggesting that they reside on a lower-dimensional manifold. In contrast, seasonal relationships involve dynamic, high-dimensional interactions like phase shifts and amplitude co-movements, requiring more expressive modeling. In this paper, we propose DMamba, a novel forecasting model that explicitly aligns architectural complexity with this component-specific characteristic. DMamba employs seasonal-trend decomposition and processes the components with specialized, differentially complex modules: a variable-direction Mamba encoder captures the rich, cross-variable dynamics within the seasonal component, while a simple Multi-Layer Perceptron (MLP) suffices to learn from the lower-dimensional inter-variable relationships in the trend component. Extensive experiments on diverse datasets demonstrate that DMamba sets a new state-of-the-art (SOTA), consistently outperforming both recent Mamba-based architectures and leading decomposition-based models.

## Keywords

Time Series Forecasting, Mamba, State Space Models, Seasonal-Trend Decomposition, Deep Learning

## 1 Introduction

Long-term time series forecasting (LTSF) is critical for real-world decision-making.

The technical landscape of LTSF has long been dominated by linear models, such as DLinear[31] and TiDE, and Transformer architectures like Autoformer[28], FEDformer[33], and PatchTST[20]. Recently, State Space Models (SSMs)[8], spearheaded by the Mamba architecture[6], have emerged as a disruptive frontier. While offering substantial computational efficiency (from  $O(L^2)$  to  $O(L)$ ), Mamba's primary advantage lies in its profound state-space reasoning. Through its content-aware selective scan, Mamba preserves global context more effectively, demonstrating a superior capacity to capture intricate dependencies that are often lost in the diffused attention mechanisms of Transformers.<sup>1</sup>

\*Both authors contributed equally to this research.

†Corresponding author.

<sup>1</sup>Source code and scripts are available at: <https://github.com/DMambaKDD/DMamba>

Following the success of iTransformer[18], prominent Mamba LTSF models tokenize each variable and use Mamba on the resulting series to model inter-channel dependence[25][17][1]. While showing promising effectiveness, current Mamba-based models frequently underperform on time series datasets with complicated non-stationarity. For example, SMamba[25] lags behind transformer-based models on Electricity Transformer Temperature (ETT) datasets. We hypothesize and validate through experiment that the degradation of performance results from the Mamba module being overwhelmed by the entanglement of multi-scale temporal patterns.

A promising paradigm to address non-stationarity and temporal complexity is to decompose raw time series into semantically distinct components, such as trend and seasonal parts, and apply separate neural networks to process them. Integration of this paradigm into various LTSF architectures, including MLP-based models[16][31] and transformer-based models [28][33], has been successful. This aligns with the statistical insight that the underlying data-generating processes for these components differ significantly. However, existing methods typically employ identical or equally complex modules for both the trend and seasonal component, thus cannot fully exploit this distinction.

We argue that the nature of inter-variable dependencies within the trend and seasonal components is inherently different, suggesting that they should be modeled with architectures of matching complexity. For example, the phenomenon of cointegration has been observed in multivariate time series data across multiple fields, including economics[4][12], finance[3][5], energy[22], environmental science[13] and transportation[11]. In cointegrated systems, the joint dynamics of the trend of variables is linearly constrained, thus can often be explained by a few common trends. In contrast, seasonal components encapsulate intricate, periodic fluctuations. The relationships between variables within a seasonal cycle can be highly dynamic, involving shifting phase alignments, amplitude co-movements, and multi-periodic interactions that are not easily captured by simple, low-dimensional representations.

Building upon the above observation, we propose **DMamba**, a novel multivariate time series forecasting model based on Decomposition and Mamba-based modeling. DMamba's design philosophy is grounded in the principle of architectural parsimony: assign complex model capacity precisely where the data complexity demands it, and use simpler models elsewhere to enhance efficiency and reduce overfitting risks. DMamba utilizes Exponential Moving Average (EMA)[15] to explicitly decouple the input into stable trend and periodic seasonal components, allowing subsequent modules to specialize. The resulting disentangled streams are then processed through a dual-flow network. A powerful Mamba-based backbone is leveraged specifically to model the purified seasonal residuals,

while the trend component is handled by a lightweight MLP. The processed representations from both pathways are integrated and passed through a forecast head to generate the final multi-step predictions.

We conduct comprehensive experiments on a wide range of benchmarks, including the ETT, Weather, and PEMS datasets. Our empirical results demonstrate that **DMamba** achieves SOTA performance, outperforming both recent Mamba-based models such as S-Mamba and leading decomposition architectures such as TimesNet and XPatch. This success is attributed to our hybrid architecture, a conclusion reinforced by extensive ablation studies. These studies demonstrate that DMamba’s superior performance stems from its strategic application of a Mamba module to complex seasonal residuals, while retaining a lightweight MLP for stable trend components. This design achieves an excellent balance and robustness, rather than solely benefiting from the robustness of the decomposition method or a specific loss function. Our contributions can be summarized as follows:

- **New Architecture:** We propose **DMamba**, a simple yet effective decomposition-based forecasting model that, explicitly aligns the complexity of the variable-relation encoder with the intrinsic statistical properties of the trend and seasonal components.
- **Theoretical Explanation:** We provide a theoretical motivation for this design from time series theory, arguing that trend relationships are often low-dimensional and thus suitable for simple MLPs, while seasonal relationships require more powerful architectures like Mamba. This insight is empirically validated by our ablation study.
- **Comprehensive Benchmarking:** Evaluations on ETT, Weather, and PEMS benchmarks demonstrate a dual breakthrough: DMamba not only sets a SOTA for Mamba-based forecasting on diverse datasets but also represents a Mamba-centric approach to outperform top-tier decomposition architectures like TimesNet and XPatch.

## 2 Related Work

Our research draws upon three primary streams of literature: Transformer-based forecasting[24], the emergence of State Space Models (SSMs)[8] in time series, and decomposition techniques.

### 2.1 Transformer-based LTSF Models

Transformers have become the dominant architecture for Long-term Time Series Forecasting (LTSF) due to their ability to model global dependencies. Early iterations focused on mitigating the  $O(L^2)$  complexity of canonical self-attention; **Informer**[32] introduced ProbSparse attention to select significant queries, while **TimesNet**[27] utilized Fourier transforms to model temporal variations in a 2D space. More recently, the focus has shifted from point-wise attention to subseries-level modeling. **PatchTST**[20] revolutionized this approach by segmenting time series into patches, enabling the model to capture local semantic information while preserving channel independence. While these architectures have achieved state-of-the-art results, they often require substantial computational resources and may struggle to distinguish essential temporal dependencies from noise in extremely long sequences.

### 2.2 Mamba for Time Series Forecasting

Recently, State Space Models (SSMs), particularly the **Mamba**[6] architecture, have emerged as a powerful alternative to Transformers, offering linear computational complexity  $O(L)$  and a hardware-aware selective scan mechanism. In the domain of time series, **S-Mamba**[25] has leveraged Mamba to capture long-range dependencies with significantly lower memory footprints than Transformers. Counterintuitively, S-Mamba models the inter-variable relationships rather than the inter-temporal relationships using the Mamba architecture, and has demonstrated superior effectiveness of the former through ablation studies. Other works, such as **Simba**[21], demonstrate Mamba’s stability in mixing channel and temporal information. However, despite their efficiency, these singular Mamba-based blocks often face challenges with non-stationary data (e.g., ETT datasets[32]). The “entanglement” of smooth trends and high-frequency fluctuations within the hidden states can degrade the selective scan’s ability to isolate stable dynamics, leading to performance degradation—a limitation our work seeks to address.

### 2.3 Decomposition and Exponential Smoothing

To mitigate non-stationarity, series decomposition has become a standard paradigm in LTSF. **Autoformer**[28] and **FEDformer**[33] integrated decomposition blocks directly into Transformer layers, while **DLinear**[31] proved that a simple linear layer applied to decomposed Trend and Seasonal components could outperform complex architectures. These methods typically rely on moving average pooling, which necessitates boundary padding and introduces distributional bias. Recent works have adopted exponential smoothing. **ETSFformer**[26] incorporates Exponential Smoothing Attention (ESA) to replace standard self-attention, while **CARD**[29] applies exponential smoothing specifically to query and key tokens within the attention head to align temporal distributions. Unlike these Transformer-centric approaches, **xPatch**[23] utilizes Exponential Moving Average (EMA)[15] as a pure decomposition module to separate trend and seasonality without padding.

In these decomposition-based methods, the trend and seasonal component are processed by models of similar complexity. A cohesive framework that explicitly aligns model capacity with the intrinsic complexity of inter-variable relationships in decomposed components—applying a powerful variable-relation encoder only where it is truly needed—remains underexplored.

## 3 Preliminaries

### 3.1 Problem Definition

We focus on the Long-term Time Series Forecasting (LTSF) task. Let  $\mathcal{X} = \{\mathbf{x}_1, \dots, \mathbf{x}_L\} \in \mathbb{R}^{L \times D}$  denote the historical look-back window, where  $L$  is the input sequence length and  $D$  represents the number of variates. The objective is to learn a mapping function  $\mathcal{F} : \mathcal{X} \rightarrow \mathcal{Y}$  to forecast the future sequence  $\mathcal{Y} = \{\mathbf{x}_{L+1}, \dots, \mathbf{x}_{L+T}\} \in \mathbb{R}^{T \times D}$ , where  $T$  is the prediction horizon.

### 3.2 State Space Models

The backbone of our proposed architecture leverages the State Space Model (SSM)[8], specifically the structured SSM used in Mamba. Conceptually, a continuous-time SSM maps a 1-D input function

or sequence  $x(t) \in \mathbb{R}$  to an output  $y(t) \in \mathbb{R}$  via a latent state  $h(t) \in \mathbb{R}^N$ . The system dynamics are governed by the following linear Ordinary Differential Equation (ODE):

$$h'(t) = Ah(t) + Bx(t), \quad y(t) = Ch(t) \quad (1)$$

where  $A \in \mathbb{R}^{N \times N}$  is the state evolution matrix[7], and  $B \in \mathbb{R}^{N \times 1}$ ,  $C \in \mathbb{R}^{1 \times N}$  are projection parameters.

To process discrete sequence data, the continuous system in Eq. (1) is discretized[9]. Adopting the Zero-Order Hold (ZOH) rule with a timescale parameter  $\Delta$ , the discrete parameters  $(\bar{A}, \bar{B})$  are derived as:

$$\bar{A} = \exp(\Delta A), \quad \bar{B} = (\Delta A)^{-1}(\exp(\Delta A) - I) \cdot \Delta B \quad (2)$$

Consequently, the discretized state equation becomes a recurrence:

$$h_t = \bar{A}h_{t-1} + \bar{B}x_t, \quad y_t = Ch_t \quad (3)$$

While Eq. (3) suggests recursive inference, modern implementations (like Mamba) utilize a hardware-aware parallel selective scan algorithm to compute this efficiently with linear complexity  $O(L)$ , serving as the fundamental building block for our seasonal modeling.

## 4 Methodology

In this section, we present the proposed **DMamba**. As shown in Figure 1, the architecture is designed to handle non-stationarity through a decouple-and-conquer strategy. The overall workflow proceeds in four stages: (1) **Normalization** via RevIN[14] to mitigate distribution shifts; (2) **Decomposition** using an Exponential Moving Average (EMA)[15] mechanism to separate trend and seasonality; (3) **Dual-flow Modeling**, where the Mamba backbone models the seasonal component while an MLP-based head models the trend; and (4) **Aggregation and Denormalization** to produce the final forecast.

### 4.1 Reversible Instance Normalization

Non-stationary time series often suffer from distribution shifts where the mean and variance change over time. To address this, we apply Reversible Instance Normalization (RevIN) before the mixing layers. Given the input batch  $X \in \mathbb{R}^{B \times L \times C}$ , we compute the instance-specific mean and standard deviation for each channel:

$$\mu = \frac{1}{L} \sum_{i=1}^L x_i, \quad \sigma = \sqrt{\frac{1}{L} \sum_{i=1}^L (x_i - \mu)^2 + \epsilon} \quad (4)$$

The input is then normalized to  $X'$ :

$$X' = \gamma \left( \frac{X - \mu}{\sigma} \right) + \beta \quad (5)$$

where  $\gamma, \beta \in \mathbb{R}^C$  are learnable affine parameters.  $\mu$  and  $\sigma$  are stored to denormalize the output later.

### 4.2 EMA-based Decomposition

The normalized input is decomposed into a **trend component** and a **seasonal component**. The trend component reflects the long-term progression and the underlying low-frequency direction of the series, effectively smoothing out short-term fluctuations. The seasonal component captures periodic patterns, high-frequency variations, and residual noise that deviate from the long-term trend.

Standard decomposition methods typically use a moving average kernel which introduces "padding bias" at boundaries. To avoid this issue, we implement an Exponential Moving Average (EMA) decomposition module. Let  $X'$  be the normalized input. The trend component  $X_{trend} \in \mathbb{R}^{L \times D}$  is computed as:

$$X_{trend}[t] = \alpha X'[t] + (1 - \alpha) X_{trend}[t-1] \quad (6)$$

The smoothing factor  $\alpha$  is a fixed hyperparameter, and for all our experiments, we set  $\alpha = 0.3$ . The seasonal component is obtained by:

$$X_{seasonal} = X' - X_{trend} \quad (7)$$

### 4.3 Dual-stream Network

The model processes the two components via separate streams to handle their distinct temporal and spatial characteristics.

**4.3.1 Seasonal Stream (Mamba Backbone).** The seasonal component  $X_{seasonal} \in \mathbb{R}^{L \times D}$  is processed by the **Mamba** backbone. Unlike traditional temporal models that scan time steps, Mamba treats each variate as a token to explicitly model inter-variate dependencies.

**Variate-wise Inverted Embedding:** For each variate  $d \in \{1, \dots, D\}$ , the entire sequence of length  $L$  is projected into a hidden space of dimension  $d_{model}$ :

$$E = \text{Embed}(X_{seasonal}) \in \mathbb{R}^{d_{model} \times D} \quad (8)$$

This inverted embedding allows the model to treat the  $D$  variates as a sequence of tokens.

**Mamba Block:** To capture inter-channel correlations while mitigating causality introduced by ordering the variables, we apply Mamba with both forward and backward directions. As shown in Figure 2, each layer in the backbone consists of a forward Mamba block ( $\text{Mamba}_{fwd}$ ) and a backward Mamba block ( $\text{Mamba}_{bwd}$ ).

The output of the bidirectional scan is fused via a residual connection:

$$H_{fwd} = \text{Mamba}_{fwd}(E), \quad H_{bwd} = \text{flip}(\text{Mamba}_{bwd}(\text{flip}(E))) \quad (9)$$

$$H_{fused} = \text{LayerNorm}(E + H_{fwd} + H_{bwd}) \quad (10)$$

Subsequently, a Feed-Forward Network (FFN), consisting of two  $1 \times 1$  convolutions and a non-linear activation  $\sigma$ , is applied:

$$H_{out} = \text{LayerNorm}(H_{fused} + \text{Dropout}(\text{Conv1d}(\sigma(\text{Conv1d}(H_{fused})))))) \quad (11)$$

Finally, the representation is projected to the prediction horizon  $T$ :

$$Y_{seasonal} = \text{Project}(H_{out}) \in \mathbb{R}^{T \times D} \quad (12)$$

**4.3.2 Trend Stream.** The trend component  $X_{trend} \in \mathbb{R}^{L \times D}$  is modeled via a channel-independent MLP to capture stable low-frequency patterns. We employ a hierarchical structure consisting of  $N$  stacked layers:

$$H_l = \text{LayerNorm}(\text{AvgPool}(W_l H_{l-1})), \quad l = 1, \dots, N \quad (13)$$

$$Y_{trend} = W_{out} H_N \in \mathbb{R}^{T \times D} \quad (14)$$

where  $H_0 = X_{trend}$ . The pooling operation  $\text{AvgPool}(\cdot)$  effectively suppresses high-frequency noise, while the linear projection  $W_{out}$  maps features to the prediction horizon  $T$ .

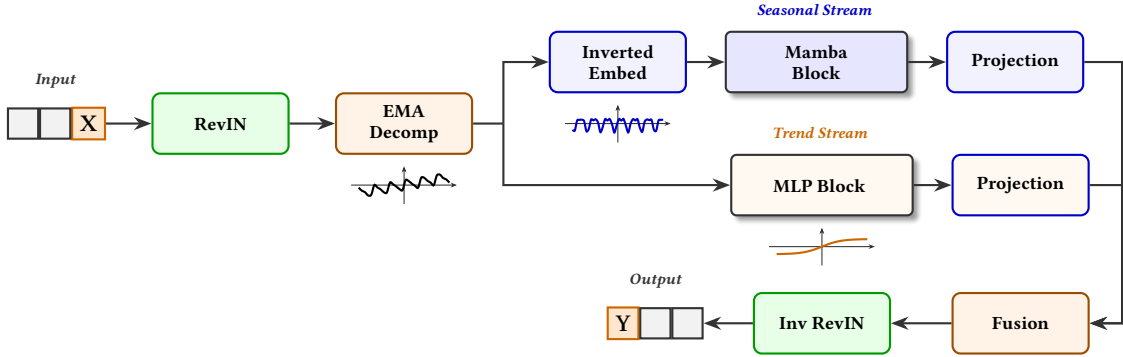


Figure 1: The Architecture of DMamba.

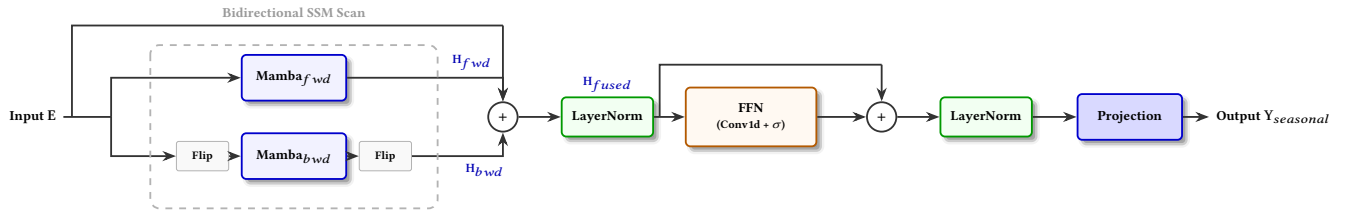


Figure 2: The Architecture of the Mamba Block.

#### 4.4 Aggregation and Denormalization

The final forecast  $\hat{Y}'_{pred}$  is produced by a linear fusion layer following the concatenation of seasonal and trend predictions:

$$\hat{Y}'_{pred} = \text{Linear}(\text{Concat}(\hat{Y}_{seasonal}, \hat{Y}_{trend})) \in \mathbb{R}^{T \times D} \quad (15)$$

We then restore the original scale using the inverse RevIN transformation:

$$\hat{Y} = \frac{\hat{Y}'_{pred} - \beta}{\gamma} \cdot \sigma + \mu \quad (16)$$

#### 4.5 Arctan Weighted Loss Function

Standard MSE/MAE losses treat all time steps equally, ignoring the increasing uncertainty over longer horizons. We use the **Arctan Weighted Loss**[29] for training to prioritize near-term accuracy. For each step  $t \in \{0, \dots, T-1\}$ , the weighting factor  $w_t$  is defined as:

$$w_t = -\arctan(t+1) + \frac{\pi}{4} + 1 \quad (17)$$

This weight monotonically decays from  $\sim 1.0$  to  $\sim 0.21$ , focusing optimization on more certain, immediate horizons. The training objective  $\mathcal{L}$  computes the weighted absolute error:

$$\mathcal{L} = \frac{1}{T \cdot D} \sum_{t=0}^{T-1} \sum_{d=1}^D w_t \cdot |\hat{y}_{t,d} - y_{t,d}| \quad (18)$$

We keep MSE/MAE losses in evaluation to ensure comparability with baseline models. For the sake of fairness, We also evaluate the performance of certain baseline models trained with Arctan Weighted Loss in Section 5.4.2.

## 5 Experiment

### 5.1 Performance on Diverse Non-stationary Benchmarks

Table 1 provides a comprehensive evaluation of DMamba against nine competitive baselines across ETT, Electricity, Exchange, and Weather datasets. The baseline suite represents three dominant paradigms in LTSF: **Mamba-based**: S-Mamba[25], TimePro[19], **Transformer-based**: iTransformer[18], PatchTST[20], FEDformer[33], TimesNet[27], and **Linear/MLP-based**: RLinear[16], DLinear[31], TiDE[2], XPatch[23].

The results demonstrate a significant breakthrough: DMamba consistently achieves SOTA performance across almost all horizons, particularly on the non-stationary ETT series. For instance, on ETTh2, DMamba outperforms *S-Mamba* by 16.5% with respect to average MSE. This validates our claim that entangled temporal patterns could overwhelm the Mamba module. Furthermore, DMamba consistently outperforms the recent baseline *TimePro* in average metrics across most datasets, particularly on the ETTh2 and Weather benchmarks, where it achieves a significant margin. Even when compared to advanced Transformers like *iTransformer* and *PatchTST*, DMamba maintains a superior edge by leveraging Mamba's content-aware selective scan on purified seasonal components. Notably, DMamba also outperforms specialized decomposition models such as *DLinear*, *XPatch*, and *FEDformer*. While these models utilize moving average or frequency-based decomposition, they often suffer from boundary padding bias or lose fine-grained temporal details. In contrast, DMamba's EMA-based dual-stream architecture ensures a more robust decoupling of stable trends and high-frequency fluctuations, setting a new benchmark for long-term forecasting.

**Table 1: We compare DMamba with 10 competitive baselines. The look-back length  $L$  is set to 96 and the forecast length  $T$  is set to {96, 192, 336, 720}. Best results are in bold, and the second best are underlined.**

Models	DMamba		S-Mamba		TimePro*		iTransformer		PatchTST		RLinear		DLinear		TiDE		FEDformer		TimesNet		XPatch		
Metric	$T$	MSE	MAE	MSE	MAE	MSE	MAE	MSE	MAE	MSE	MAE	MSE	MAE	MSE	MAE	MSE	MAE	MSE	MAE	MSE	MAE		
ETTh1	96	0.377	<b>0.390</b>	0.386	0.405	—	—	0.386	0.405	0.414	0.419	0.386	0.395	0.386	0.400	0.479	0.464	<b>0.376</b>	0.419	0.384	0.402	0.425	0.427
	192	<b>0.414</b>	<b>0.407</b>	0.443	0.437	—	—	0.441	0.436	0.460	0.445	0.437	<u>0.424</u>	0.437	0.432	0.525	0.492	<u>0.420</u>	0.448	0.436	0.429	0.436	0.425
	336	<u>0.441</u>	<u>0.427</u>	0.489	0.468	—	—	0.487	<u>0.458</u>	0.501	0.466	0.479	0.446	0.481	0.459	0.565	0.515	<u>0.459</u>	0.465	0.491	0.469	0.454	0.433
	720	<b>0.465</b>	<b>0.457</b>	0.502	0.489	—	—	0.503	0.491	0.500	0.488	0.481	0.470	0.519	0.516	0.594	0.558	0.506	0.507	0.521	0.500	<u>0.478</u>	0.461
	Avg	<b>0.424</b>	<b>0.420</b>	0.455	0.450	<u>0.438</u>	0.438	0.454	0.447	0.469	0.454	0.446	0.434	0.456	0.452	0.541	0.507	0.440	0.460	0.458	0.450	0.448	0.437
ETTh2	96	<b>0.235</b>	<b>0.301</b>	0.296	0.348	—	—	0.297	0.349	0.302	0.348	0.288	0.338	0.333	0.387	0.400	0.440	0.358	0.397	0.340	0.374	0.237	0.307
	192	<b>0.291</b>	<b>0.335</b>	0.376	0.396	—	—	0.380	0.400	0.388	0.400	<u>0.374</u>	<u>0.390</u>	0.477	0.476	0.528	0.509	0.429	0.439	0.402	0.414	<u>0.293</u>	0.341
	336	<u>0.342</u>	<u>0.374</u>	0.424	0.431	—	—	0.428	0.432	0.426	0.433	<b>0.415</b>	<u>0.426</u>	0.594	0.541	0.643	0.571	0.496	0.487	0.452	0.452	<b>0.340</b>	0.376
	720	<u>0.404</u>	<u>0.425</u>	0.426	0.444	—	—	0.427	0.445	0.431	0.446	<b>0.420</b>	<u>0.440</u>	0.831	0.657	0.874	0.679	0.463	0.474	0.462	0.468	<b>0.403</b>	0.426
	Avg	<b>0.318</b>	<b>0.359</b>	0.381	0.405	<u>0.377</u>	0.403	0.383	0.407	0.387	0.407	0.374	0.398	0.559	0.515	0.611	0.550	0.437	0.449	0.414	0.427	<b>0.318</b>	0.363
ETTm1	96	<b>0.307</b>	<b>0.345</b>	0.333	0.368	—	—	0.334	0.368	0.329	0.367	0.355	0.376	0.345	0.372	0.364	0.387	0.379	0.419	0.338	0.375	0.323	0.354
	192	<b>0.350</b>	<b>0.372</b>	0.376	0.390	—	—	0.377	0.391	<u>0.367</u>	<u>0.385</u>	0.391	0.392	0.380	0.389	0.398	0.404	0.426	0.441	0.374	0.387	<u>0.356</u>	0.372
	336	<b>0.385</b>	<b>0.391</b>	0.408	0.413	—	—	0.426	0.420	<u>0.399</u>	<u>0.410</u>	0.424	<u>0.415</u>	0.413	0.413	0.428	0.425	0.445	0.459	0.410	0.411	<u>0.394</u>	0.395
	720	<u>0.462</u>	<u>0.430</u>	0.475	0.448	—	—	0.491	0.459	<b>0.454</b>	<u>0.439</u>	0.487	0.450	<u>0.474</u>	0.453	0.487	0.461	0.543	0.490	0.478	0.450	0.465	<b>0.430</b>
	Avg	<b>0.376</b>	<b>0.385</b>	0.398	0.405	0.391	<u>0.400</u>	0.407	0.410	<u>0.387</u>	<u>0.400</u>	0.414	0.407	0.403	0.407	0.419	0.419	0.448	0.452	0.400	0.406	<u>0.385</u>	0.388
ETTm2	96	<b>0.164</b>	<b>0.247</b>	0.179	0.263	—	—	0.180	0.264	0.175	0.259	0.182	0.265	0.193	0.292	0.207	0.305	0.203	0.287	0.187	0.267	0.167	0.250
	192	<b>0.229</b>	<b>0.291</b>	0.250	0.309	—	—	0.250	0.309	0.241	<u>0.302</u>	0.246	0.304	0.284	0.362	0.290	0.364	0.269	0.328	0.249	0.309	<u>0.231</u>	0.292
	336	<b>0.292</b>	<b>0.331</b>	0.312	0.349	—	—	0.311	0.348	0.305	0.343	<u>0.307</u>	<u>0.342</u>	0.369	0.427	0.377	0.422	0.325	0.366	0.321	0.351	<b>0.292</b>	0.332
	720	<b>0.380</b>	<b>0.384</b>	0.411	0.406	—	—	0.412	0.407	<u>0.402</u>	<u>0.400</u>	0.407	<u>0.398</u>	0.554	0.522	0.558	0.524	0.421	0.415	0.408	0.403	<b>0.380</b>	0.385
	Avg	<b>0.266</b>	<b>0.313</b>	0.288	0.332	<u>0.281</u>	<u>0.326</u>	0.288	0.332	<u>0.281</u>	<u>0.326</u>	0.286	<u>0.327</u>	0.350	0.401	0.358	0.404	0.305	0.349	0.291	0.333	<u>0.267</u>	0.314
Elec.	96	0.144	<b>0.233</b>	<b>0.139</b>	0.235	—	—	0.148	0.240	0.181	0.270	0.201	0.281	0.197	0.282	0.237	0.329	0.193	0.308	0.168	0.272	0.192	0.267
	192	<b>0.156</b>	<b>0.245</b>	0.159	0.255	—	—	0.162	<u>0.253</u>	0.188	0.274	0.201	0.283	0.196	0.285	0.236	0.330	0.201	0.315	0.184	0.289	0.190	0.269
	336	<b>0.172</b>	<b>0.261</b>	0.176	0.272	—	—	0.178	<u>0.269</u>	0.204	0.293	0.215	0.298	0.209	0.301	0.249	0.344	0.214	0.329	0.198	0.300	0.206	0.284
	720	<u>0.206</u>	<b>0.293</b>	<b>0.204</b>	0.298	—	—	0.225	0.317	0.246	0.324	0.257	0.331	0.245	0.333	0.284	0.373	0.246	0.355	<u>0.220</u>	0.320	0.244	0.314
	Avg	<u>0.170</u>	<u>0.258</u>	<u>0.170</u>	0.265	<b>0.169</b>	<b>0.262</b>	0.178	0.270	0.205	0.290	0.219	0.298	0.212	0.300	0.251	0.344	0.214	0.327	0.192	0.295	0.208	0.284
Exch.	96	0.080	<b>0.198</b>	<b>0.086</b>	0.207	—	—	<b>0.086</b>	0.206	0.088	0.205	0.093	0.217	0.088	0.218	0.094	0.218	0.148	0.278	0.107	0.234	0.085	0.202
	192	<b>0.171</b>	<b>0.294</b>	0.182	0.304	—	—	0.177	0.299	<u>0.176</u>	<u>0.299</u>	0.184	0.307	<u>0.176</u>	0.315	0.184	0.307	0.271	0.315	0.226	0.344	0.177	0.298
	336	<u>0.337</u>	<u>0.418</u>	0.332	0.418	—	—	<u>0.331</u>	<u>0.417</u>	<b>0.301</b>	<b>0.397</b>	0.351	0.432	<u>0.313</u>	0.427	0.349	0.431	0.460	0.427	0.367	0.448	0.345	0.422
	720	<b>0.847</b>	0.693	<u>0.867</u>	0.703	—	—	<b>0.847</b>	<u>0.691</u>	0.901	0.714	0.886	0.714	<u>0.839</u>	<b>0.695</b>	0.852	0.698	1.195	<b>0.695</b>	0.964	0.746	0.877	0.707
	Avg	0.359	<u>0.401</u>	0.367	0.408	<b>0.352</b>	<b>0.399</b>	0.360	<u>0.403</u>	0.367	<u>0.404</u>	0.378	0.417	<u>0.354</u>	0.414	0.370	0.413	0.519	0.429	0.416	0.443	0.371	0.407
Weath.	96	0.166	<b>0.201</b>	<b>0.165</b>	0.210	—	—	0.174	0.214	0.177	0.218	0.192	0.232	0.196	0.255	0.202	0.261	0.217	0.296	0.172	0.220	0.190	0.222
	192	0.216	<b>0.247</b>	<b>0.214</b>	0.252	—	—	0.221	<u>0.254</u>	0.225	0.259	0.240	0.271	0.237	0.296	0.242	0.298	0.276	0.336	0.219	0.261	0.232	0.257
	336	<b>0.240</b>	<b>0.278</b>	0.274	0.297	—	—	0.278	0.296	<u>0.278</u>	<u>0.297</u>	0.292	0.307	<u>0.283</u>	0.335	0.287	0.335	0.339	0.380	0.280	0.306	<u>0.248</u>	0.280
	720	<b>0.316</b>	<u>0.330</u>	0.350	0.345	—	—	0.358	0.347	0.354	0.348	0.364	0.353	<u>0.345</u>	0.381	0.351	0.386	0.403	0.428	0.365	0.359	<u>0.318</u>	<b>0.326</b>
	Avg	<b>0.234</b>	<b>0.264</b>	<u>0.251</u>	0.276	<u>0.251</u>	0.276	0.258	0.278	0.259	0.282	0.272	0.291	0.265	0.317	0.271	0.320	0.309	0.360	0.259	0.287	<u>0.247</u>	0.271

\* The original paper of TimePro does not provide specific metrics for each forecast length.

## 5.2 Performance on PEMS Datasets

To further assess spatial-temporal modeling capabilities, we evaluate DMamba on the PEMS (03, 04, 07, 08)[30][10] benchmarks, which are characterized by high-dimensional variates and strong periodicity. As shown in Table 2, DMamba yields consistent improvements even in scenarios where baselines like *S-Mamba* and *iTransformer* traditionally perform well.

Compared to MLP-based architectures such as *TiDE* and linear mappings like *RLinear* and *DLinear*—which often struggle with the complex, non-linear dependencies in traffic flow—DMamba

exhibits superior stability. For example, on the PEMS08 dataset, DMamba reduces the average MSE from 0.148 (*S-Mamba*) and 0.150 (*iTransformer*) to an impressive 0.099, representing a 33.1% improvement over its Mamba-based predecessor. Even against *TimesNet* and *PatchTST*, which excel at capturing local patterns, DMamba provides more accurate long-range forecasts. This success is attributed to the synergistic effect of the dual-stream network: while the trend stream handles stable shifts, the Mamba-based seasonal stream captures intricate inter-variate correlations free from the interference

**Table 2: Full results on PEMS datasets. We compare DMamba with 9 competitive baselines. The look-back length  $L$  is set to 96 and the forecast length  $T$  is set to  $\{12, 24, 48, 96\}$ . Best results are in bold, and the second best are underlined.**

Models	<b>DMamba</b>	S-Mamba		iTransformer		PatchTST		RLinear		DLinear		TiDE		FEDformer		TimesNet		XPatch			
Metric	$T$	MSE	MAE	MSE	MAE	MSE	MAE	MSE	MAE	MSE	MAE	MSE	MAE	MSE	MAE	MSE	MAE	MSE	MAE		
PEMS03	12	<b>0.060</b>	<b>0.161</b>	0.065	0.169	0.071	0.174	0.099	0.216	0.126	0.236	0.122	0.243	0.178	0.305	0.126	0.251	0.085	0.192	0.090	0.197
	24	<b>0.077</b>	<b>0.183</b>	0.087	0.196	0.093	0.201	0.142	0.259	0.246	0.334	0.201	0.317	0.257	0.371	0.149	0.275	0.118	0.223	0.140	0.248
	48	<b>0.109</b>	<b>0.217</b>	0.133	0.243	0.125	0.236	0.211	0.319	0.551	0.529	0.333	0.425	0.379	0.463	0.227	0.348	0.155	0.260	0.255	0.338
	96	<b>0.147</b>	<b>0.256</b>	0.201	0.305	0.164	0.275	0.269	0.370	1.057	0.787	0.457	0.515	0.490	0.539	0.348	0.434	0.228	0.317	0.380	0.423
Avg		<b>0.098</b>	<b>0.204</b>	0.122	0.228	0.113	0.221	0.180	0.291	0.495	0.472	0.278	0.375	0.326	0.419	0.213	0.327	0.147	0.248	0.216	0.301
PEMS04	12	<b>0.074</b>	<b>0.174</b>	0.076	0.180	0.078	0.183	0.105	0.224	0.138	0.252	0.148	0.272	0.219	0.340	0.138	0.262	0.087	0.195	0.106	0.214
	24	0.089	0.194	<b>0.084</b>	<b>0.193</b>	0.095	0.205	0.153	0.275	0.258	0.348	0.224	0.340	0.292	0.398	0.177	0.293	0.103	0.215	0.168	0.274
	48	<b>0.113</b>	<b>0.220</b>	0.115	0.224	0.120	0.233	0.229	0.339	0.572	0.544	0.355	0.437	0.409	0.478	0.270	0.368	0.136	0.250	0.308	0.375
	96	0.143	0.251	<b>0.137</b>	<b>0.248</b>	0.150	0.262	0.291	0.389	1.137	0.820	0.452	0.504	0.492	0.532	0.341	0.427	0.190	0.303	0.491	0.492
Avg		0.105	<b>0.210</b>	<b>0.103</b>	<b>0.211</b>	0.111	0.221	0.195	0.307	0.526	0.491	0.295	0.388	0.353	0.437	0.231	0.337	0.129	0.241	0.268	0.339
PEMS07	12	<b>0.059</b>	<b>0.150</b>	0.063	<b>0.159</b>	0.067	0.165	0.095	0.207	0.118	0.235	0.115	0.242	0.173	0.304	0.109	0.225	0.082	0.181	0.083	0.189
	24	<b>0.077</b>	<b>0.173</b>	0.081	<b>0.183</b>	0.088	0.190	0.150	0.262	0.242	0.341	0.210	0.329	0.271	0.383	0.125	0.244	0.101	0.204	0.138	0.244
	48	0.096	0.198	<b>0.093</b>	<b>0.192</b>	0.110	0.215	0.253	0.340	0.562	0.541	0.398	0.458	0.446	0.495	0.165	0.288	0.134	0.238	0.265	0.342
	96	0.131	0.234	<b>0.117</b>	<b>0.217</b>	0.139	0.245	0.346	0.404	1.096	0.795	0.594	0.553	0.628	0.577	0.262	0.376	0.181	0.279	0.443	0.453
Avg		0.091	0.189	<b>0.089</b>	<b>0.188</b>	0.101	0.204	0.211	0.303	0.504	0.478	0.329	0.395	0.380	0.440	0.165	0.283	0.124	0.225	0.232	0.307
PEMS08	12	<b>0.067</b>	<b>0.163</b>	0.076	0.178	0.079	0.182	0.168	0.232	0.133	0.247	0.154	0.276	0.227	0.343	0.173	0.273	0.112	0.212	0.097	0.204
	24	<b>0.080</b>	<b>0.180</b>	0.104	<b>0.209</b>	0.115	0.219	0.224	0.281	0.249	0.343	0.248	0.353	0.318	0.409	0.210	0.301	0.141	0.238	0.157	0.262
	48	<b>0.103</b>	<b>0.205</b>	0.167	<b>0.228</b>	0.186	0.235	0.321	0.354	0.569	0.544	0.440	0.470	0.497	0.510	<b>0.320</b>	0.394	0.198	0.283	0.281	0.357
	96	<b>0.145</b>	<b>0.248</b>	0.245	<b>0.280</b>	0.221	<b>0.267</b>	0.408	0.417	1.166	0.814	0.674	0.565	0.721	0.592	0.442	0.465	0.320	0.351	0.487	0.477
Avg		<b>0.099</b>	<b>0.199</b>	0.148	<b>0.224</b>	0.150	0.226	0.280	0.321	0.529	0.487	0.379	0.416	0.441	0.464	0.286	0.358	0.193	0.271	0.255	0.325

of low-frequency noise. These consistent gains across PEMS benchmarks solidify DMamba’s position as a superior general-purpose architecture for multivariate time series forecasting.

### 5.3 Efficiency Analysis

We evaluate the trade-off between predictive accuracy (Avg MSE), inference latency, and computational cost (FLOPs), as shown in Figure 3. **DMamba** consistently occupies the optimal bottom-left quadrant, demonstrating a superior balance of high accuracy and efficiency. For instance, on PEMS03, DMamba is nearly **9x faster** than PatchTST (10ms vs. 90ms) and over **10x lighter** in FLOPs (0.32G vs. 3.60G), while achieving a lower MSE. This advantage stems from our hybrid design, which pairs the linear-time complexity of Mamba with a lightweight MLP, outperforming both high-latency Transformers and less accurate fast models.

### 5.4 Ablation Study

**5.4.1 Ablation Study on Branch Architectures across ETT Datasets.** To evaluate the individual contributions of our hybrid design, we compare the proposed **DMamba** with four architectural variants: **All-MLP** (MLP for both branches), **Mamba-Trend** (MLP for Seasonal, Mamba for Trend), **All-Mamba** (Mamba for both branches), and **T-Mamba** (Temporal Mamba for Seasonal). The results summarized in Table 3 demonstrate that **DMamba** consistently achieves the lowest average MSE and MAE across all four ETT benchmarks. This validates our core strategy of utilizing high-capacity Mamba

blocks for purified seasonal residuals while maintaining a stable MLP for trend projections to ensure overall robustness.

Analysis of individual datasets reveals that while **All-MLP** remains competitive on the relatively stable ETTh1 dataset—securing the best results for specific horizons such as  $T = 96$  and  $T = 720$ —it generally lacks the representational power to model more complex temporal fluctuations. By introducing the Mamba block into the seasonal stream, **DMamba** effectively captures non-linear periodicities, leading to a substantial performance boost in the more non-stationary ETTh2 dataset. This confirms that the selective scan mechanism of Mamba is particularly potent when applied to high-frequency seasonal components.

The suboptimality of the **Mamba-Trend** configuration further reinforces our architectural choice. By assigning the Mamba block to the trend branch and an MLP to the seasonal branch, performance degrades significantly across almost all tested horizons. For instance, the average MSE for Mamba-Trend on ETTh2 is 0.355, which is notably inferior to **DMamba**’s 0.318. This clear performance gap demonstrates that the state-space paradigm is fundamentally better suited to process seasonal residuals than to model inter-channel correlations among trend components.

Furthermore, we evaluate **T-Mamba**, where the Mamba block scans along the temporal dimension rather than the variate dimension. **DMamba** surpasses **T-Mamba** across most metrics (e.g., improving Avg MSE from 0.365 to 0.318 on ETTh2), indicating that explicitly modeling inter-variety dependencies via channel-wise

**Table 3: Ablation Study on Branch Architectures across ETT Datasets.** We evaluate the effectiveness of the Mamba block by placing it in different branches: **DMamba** (Mamba for Seasonal, MLP for Trend), **All-MLP** (MLP for both), **Mamba-Trend** (MLP for Seasonal, Mamba for Trend), **All-Mamba** (Mamba for both), and **T-Mamba** (Temporal Mamba for Seasonal). Best results are in **bold**, and the second best are **underlined**.

Models	<b>DMamba</b>		All-MLP		Mamba-Trend		All-Mamba		T-Mamba		
	Dataset	T	MSE	MAE	MSE	MAE	MSE	MAE	MSE	MAE	
ETTh1	96	<u>0.377</u>	<u>0.390</u>	<u>0.376</u>	<u>0.392</u>	0.379	0.398	0.377	0.394	0.380	0.396
	192	<b>0.414</b>	<b>0.407</b>	0.430	0.418	0.435	0.426	<u>0.431</u>	<u>0.421</u>	0.437	0.423
	336	<b>0.441</b>	<b>0.427</b>	<u>0.471</u>	<u>0.437</u>	0.477	0.445	0.472	0.440	0.484	0.442
	720	<u>0.465</u>	<u>0.457</u>	<b>0.461</b>	<b>0.459</b>	0.482	0.467	0.471	0.461	0.498	0.468
<b>Avg</b>		<b>0.424</b>	<b>0.421</b>	0.435	0.427	0.443	0.434	0.438	0.429	0.449	0.432
ETTh2	96	<b>0.235</b>	<b>0.301</b>	0.294	0.338	0.288	0.336	<u>0.285</u>	<u>0.333</u>	0.298	0.339
	192	<b>0.291</b>	<b>0.335</b>	0.371	0.386	0.361	0.382	<u>0.358</u>	<u>0.379</u>	0.367	0.384
	336	<b>0.342</b>	<b>0.374</b>	0.379	0.402	<u>0.371</u>	<u>0.397</u>	0.374	0.399	0.380	0.403
	720	0.404	0.425	0.411	0.430	<u>0.398</u>	<u>0.422</u>	<b>0.393</b>	<b>0.417</b>	0.414	0.432
<b>Avg</b>		<b>0.318</b>	<b>0.359</b>	0.364	0.389	0.355	0.384	<u>0.353</u>	<u>0.382</u>	0.365	0.389
ETTm1	96	<b>0.307</b>	<b>0.345</b>	0.327	0.348	0.326	0.352	0.319	<b>0.345</b>	0.317	<b>0.345</b>
	192	<b>0.350</b>	<b>0.372</b>	0.374	<u>0.371</u>	0.369	0.374	0.369	0.372	0.371	0.374
	336	<b>0.385</b>	<b>0.391</b>	0.405	0.392	0.400	0.394	0.401	0.394	0.390	0.392
	720	<b>0.462</b>	<b>0.430</b>	0.467	<b>0.429</b>	0.480	0.438	0.470	0.434	0.455	<b>0.429</b>
<b>Avg</b>		<b>0.376</b>	<b>0.385</b>	0.393	0.385	0.394	0.390	0.390	0.386	<u>0.383</u>	<u>0.385</u>
ETTm2	96	<b>0.164</b>	<b>0.247</b>	0.179	0.255	0.173	0.252	<u>0.172</u>	<u>0.252</u>	0.175	0.253
	192	<b>0.229</b>	<b>0.291</b>	0.243	0.297	0.242	0.298	<u>0.239</u>	<u>0.295</u>	0.240	0.296
	336	<b>0.292</b>	<b>0.331</b>	0.300	<u>0.334</u>	0.299	0.335	0.304	0.337	0.303	0.335
	720	<b>0.380</b>	<b>0.384</b>	0.395	<u>0.391</u>	0.400	0.394	0.398	0.392	0.400	0.393
<b>Avg</b>		<b>0.266</b>	<b>0.313</b>	0.279	0.319	0.279	0.320	<u>0.278</u>	<u>0.319</u>	0.279	<u>0.319</u>

scanning is more critical than temporal scanning for capturing the dynamic interactions within seasonal fluctuations.

Finally, although the **All-Mamba** variant shows strong modeling capacity and achieves the best MSE on the ETTh2 horizon of  $T = 720$ , its performance on longer horizons in ETTm1 and ETTm2 is less consistent compared to **DMamba**. This suggests that over-parameterizing the trend component with a high-capacity state-space model may lead to the capture of spurious correlations. **DMamba** maintains a superior balance by utilizing the MLP as a robust inductive bias for trend modeling, which prevents overfitting and enhances generalization across diverse non-stationary sequences. Consequently, the hybrid configuration of **DMamba** proves to be the most reliable architecture for robust long-term forecasting.

**5.4.2 Ablation Study on the Arctan Weighted Loss for DMamba.** To verify that the superior performance of **DMamba** stems from its architectural design rather than solely from the choice of loss function, we conduct a controlled experiment by equipping all models with the same **Arctan Weighted Loss**. We deliberately selected four of the most competitive recent baselines—S-Mamba, PatchTST, iTransformer, and xPatch—which represent the state-of-the-art in State Space Models, Transformers, and linear-based architectures.

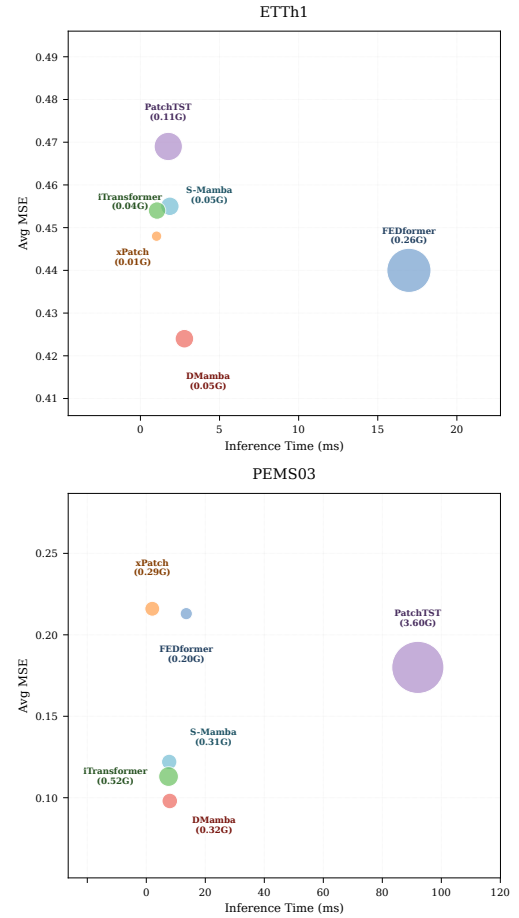


**Figure 3: Efficiency trade-off on ETTh1 and PEM03 with a look-back window of  $L = 96$ .** **DMamba** (bottom-left) achieves the best balance of low error (Avg MSE), fast inference, and low computational cost (FLOPs, bubble size).

In Table 4, models marked with an asterisk (\*) indicate that their original uniform MSE objective has been replaced by this weighted loss. This setup ensures a fair comparison where the loss function is a controlled variable across these highly competitive backbones.

The results demonstrate that while the Arctan Weighted Loss is a vital component of the **DMamba** framework, it does not compensate for the structural limitations of other architectures. Even when utilizing the same temporal prioritization, **DMamba**\* consistently outperforms these strong baselines. This confirms that our architectural synergy—the combination of EMA-based decomposition and Mamba-based seasonal modeling—is the primary driver of robustness, with the specialized loss function serving as a complementary enhancement to this structural core.

**5.4.3 Ablation Study on the Sensitivity Analysis of EMA Smoothing Factor.** Our sensitivity analysis of the EMA smoothing factor  $\alpha$  across ETT datasets shows its optimal value is data-dependent. ETTh1 benefits from a higher  $\alpha$  (0.7) for agile adaptation, while

**Table 4: Performance comparison under a unified Arctan Weighted Loss across competitive baselines. Models marked with an asterisk (\*) denote that their native uniform MSE loss has been substituted with the proposed weighted loss. Bold indicates the best performance, and underlined indicates the second best.**

Dataset	Metric	Models with Arctan Weighted Loss (*)				
		DMamba*	S-Mamba*	PatchTST*	iTransformer*	xPatch*
ETTh1	MSE	<b>0.431</b>	0.471	<u>0.446</u>	0.448	0.448
	MAE	<b>0.426</b>	0.451	<u>0.432</u>	0.439	0.437
ETTh2	MSE	<b>0.318</b>	0.371	0.362	0.380	<b>0.318</b>
	MAE	<b>0.359</b>	0.392	0.388	0.398	<u>0.363</u>
ETTm1	MSE	<b>0.376</b>	0.403	<u>0.382</u>	0.398	0.385
	MAE	<u>0.385</u>	0.397	<b>0.380</b>	0.393	0.388
ETTm2	MSE	<b>0.266</b>	0.282	0.281	0.283	<u>0.268</u>
	MAE	<b>0.313</b>	0.322	0.319	0.322	<u>0.315</u>

$\alpha = 0.3$  proved most robust for ETTh2, ETTm1, and ETTm2, effectively balancing trend stability and responsiveness. The EMA decomposition module demonstrates overall robustness within  $\alpha \in [0.3, 0.7]$ . Detailed results are in Table 5 in the appendix.

## References

[1] Md Atik Ahamed and Qiang Cheng. 2024. Timemachine: A time series is worth 4 mambas for long-term forecasting. In *ECAI 2024: 27th European Conference on Artificial Intelligence, 19-24 October 2024, Santiago de Compostela, Spain-Including 13th Conference on Prestigious Applications of Intelligent Systems. European Conference on Artificial Intelli*, Vol. 392. 1688.

[2] Abhimanyu Das, Weihao Kong, Andrew Leach, Shaan Mathur, Rajat Sen, and Rose Yu. 2023. Long-term forecasting with tide: Time-series dense encoder. *arXiv preprint arXiv:2304.08424* (2023).

[3] Gerald P Dwyer Jr and Myles S Wallace. 1992. Cointegration and market efficiency. *Journal of International Money and Finance* 11, 4 (1992), 318–327.

[4] Robert F Engle and Clive WJ Granger. 1987. Co-integration and error correction: representation, estimation, and testing. *Econometrica: journal of the Econometric Society* (1987), 251–276.

[5] Evan Gatev, William N Goetzmann, and K Geert Rouwenhorst. 2006. Pairs trading: Performance of a relative-value arbitrage rule. *The review of financial studies* 19, 3 (2006), 797–827.

[6] Albert Gu and Tri Dao. 2024. Mamba: Linear-time sequence modeling with selective state spaces. In *First conference on language modeling*.

[7] Albert Gu, Stefano Ermon, Atri Rudra, and Christopher Ré. 2020. Hippo: Recurrent memory with optimal polynomial projections. *Advances in neural information processing systems* 33 (2020), 1474–1487.

[8] Albert Gu, Karan Goel, and Christopher Ré. 2021. Efficiently modeling long sequences with structured state spaces. *arXiv preprint arXiv:2111.00396* (2021).

[9] Albert Gu, Isys Johnson, Karan Goel, Khaled Saab, Tri Dao, Atri Rudra, and Christopher Ré. 2021. Combining recurrent, convolutional, and continuous-time models with linear state space layers. *Advances in neural information processing systems* 34 (2021), 572–585.

[10] Shengnan Guo, Youfang Lin, Ning Feng, Chao Song, and Huaiyu Wan. 2019. Attention based spatial-temporal graph convolutional networks for traffic flow forecasting. In *Proceedings of the AAAI conference on artificial intelligence*, Vol. 33. 922–929.

[11] Ryo Inoue and Akihisa Miyashita. 2021. Short-term traffic speed prediction based on fundamental and cointegration relationship of speed-density in non-congested and congested states. *IEEE Open Journal of Intelligent Transportation Systems* 2 (2021), 470–481.

[12] Soren Johansen and Katarina Juselius. 1990. Maximum likelihood estimation and inference on cointegration—with applications to the demand for money. *Oxford Bulletin of Economics and statistics* 52, 2 (1990), 169–210.

[13] Robert K Kaufmann and David I Stern. 2002. Cointegration analysis of hemispheric temperature relations. *Journal of Geophysical Research: Atmospheres* 107, D2 (2002), ACL-8.

[14] Taesung Kim, Jinhee Kim, Yunwon Tae, Cheonbok Park, Jang-Ho Choi, and Jaegul Choo. 2021. Reversible instance normalization for accurate time-series forecasting against distribution shift. In *International conference on learning representations*.

[15] AJ Lawrence and PAW Lewis. 1977. An exponential moving-average sequence and point process (EMA1). *Journal of Applied Probability* 14, 1 (1977), 98–113.

[16] Zhe Li, Shiyi Qi, Yiduo Li, and Zenglin Xu. 2023. Revisiting long-term time series forecasting: An investigation on linear mapping. *arXiv preprint arXiv:2305.10721* (2023).

[17] Aobo Liang, Xingguo Jiang, Yan Sun, Xiaohou Shi, and Ke Li. 2024. Bi-mamba+: Bidirectional mamba for time series forecasting. *arXiv preprint arXiv:2404.15772* (2024).

[18] Yong Liu, Tengge Hu, Haoran Zhang, Haixu Wu, Shiyu Wang, Lintao Ma, and Mingsheng Long. 2023. itransformer: Inverted transformers are effective for time series forecasting. *arXiv preprint arXiv:2310.06625* (2023).

[19] Xiaowen Ma, Zhenliang Ni, Shuai Xiao, and Xinghao Chen. 2025. TimePro: Efficient Multivariate Long-term Time Series Forecasting with Variable-and Time-Aware Hyper-state. *arXiv preprint arXiv:2505.20774* (2025).

[20] Y Nie. 2022. A Time Series is Worth 64Words: Long-term Forecasting with Transformers. *arXiv preprint arXiv:2211.14730* (2022).

[21] Badri N Patro and Vijay S Agneeswaran. 2024. Simba: Simplified mamba-based architecture for vision and multivariate time series. *arXiv preprint arXiv:2403.15360* (2024).

[22] Boriss Siliverstovs, Guillaume L'Hégaret, Anne Neumann, and Christian Von Hirschhausen. 2005. International market integration for natural gas? A cointegration analysis of prices in Europe, North America and Japan. *Energy Economics* 27, 4 (2005), 603–615.

[23] Artyom Stitsyuk and Jaesik Choi. 2025. xPatch: Dual-Stream Time Series Forecasting with Exponential Seasonal-Trend Decomposition. In *Proceedings of the AAAI Conference on Artificial Intelligence*, Vol. 39. 20601–20609.

[24] Liyilei Su, Xumin Zuo, Rui Li, Xin Wang, Heng Zhao, and Bingding Huang. 2025. A systematic review for transformer-based long-term series forecasting. *Artificial Intelligence Review* 58, 3 (2025), 80.

[25] Zihan Wang, Fanheng Kong, Shi Feng, Ming Wang, Xiaocui Yang, Han Zhao, Daling Wang, and Yifei Zhang. 2025. Is mamba effective for time series forecasting? *Neurocomputing* 619 (2025), 129178.

[26] Gerald Woo, Chenghao Liu, Doyen Sahoo, Akshat Kumar, and Steven Hoi. 2022. Etsformer: Exponential smoothing transformers for time-series forecasting. *arXiv preprint arXiv:2202.01381* (2022).

[27] Haixi Wu, Tengge Hu, Yong Liu, Hang Zhou, Jianmin Wang, and Mingsheng Long. 2022. Timesnet: Temporal 2d-variation modeling for general time series analysis. *arXiv preprint arXiv:2210.02186* (2022).

[28] Haixi Wu, Jiehui Xu, Jianmin Wang, and Mingsheng Long. 2021. Autoformer: Decomposition transformers with auto-correlation for long-term series forecasting. *Advances in neural information processing systems* 34 (2021), 22419–22430.

[29] Wang Xue, Tian Zhou, Qingsong Wen, Jinyang Gao, Bolin Ding, and Rong Jin. 2023. Card: Channel aligned robust blend transformer for time series forecasting. *arXiv preprint arXiv:2305.12095* (2023).

[30] Bing Yu, Haoteng Yin, and Zhanxing Zhu. 2017. Spatio-temporal graph convolutional networks: A deep learning framework for traffic forecasting. *arXiv preprint arXiv:1709.04875* (2017).

[31] Ailing Zeng, Muxi Chen, Lei Zhang, and Qiang Xu. 2023. Are transformers effective for time series forecasting? In *Proceedings of the AAAI conference on artificial intelligence*, Vol. 37. 11121–11128.

[32] Haoyi Zhou, Shanghang Zhang, Jieqi Peng, Shuai Zhang, Jianxin Li, Hui Xiong, and Wancai Zhang. 2021. Informer: Beyond efficient transformer for long sequence time-series forecasting. In *Proceedings of the AAAI conference on artificial intelligence*, Vol. 35. 11106–11115.

[33] Tian Zhou, Ziqing Ma, Qingsong Wen, Xue Wang, Liang Sun, and Rong Jin. 2022. Fedformer: Frequency enhanced decomposed transformer for long-term series forecasting. In *International conference on machine learning*. PMLR, 27268–27286.

## A Ablation Study on the Sensitivity Analysis of EMA Smoothing Factor

To investigate the impact of the EMA smoothing factor  $\alpha$  on forecasting performance, we conduct a sensitivity analysis across all ETT datasets. The smoothing factor  $\alpha$  is a critical hyperparameter that dictates the trade-off between trend stability and responsiveness. As shown in Table 5, the optimal value for  $\alpha$  varies slightly depending on the data characteristics.

For the ETTh1 dataset, a larger smoothing factor ( $\alpha = 0.7$ ) achieves the best performance, indicating that this dataset benefits from a more agile trend adaptation that can quickly respond to shifts. In contrast, for ETTh2, ETTm1, and ETTm2, the baseline value of  $\alpha = 0.3$  remains the most robust choice, consistently

yielding the lowest MSE and MAE. This suggests that for many non-stationary scenarios, a moderate  $\alpha$  effectively prevents the trend component from over-fitting to high-frequency noise while still capturing long-term shifts. The relatively stable performance across the range of  $\alpha \in [0.3, 0.7]$  demonstrates the inherent robustness of our EMA-based decomposition module.

**Table 5: Sensitivity analysis of the EMA smoothing factor  $\alpha$  across ETT datasets ( $L = 96, T = 96$ ). We evaluate the performance impact of different  $\alpha$  values. Bold indicates the best performance, and underlined indicates the second best.**

Dataset	Metric	Smoothing Factor $\alpha$					Best $\alpha$
		0.1	0.3	0.5	0.7	0.9	
ETTh1	MSE	0.380	0.377	<u>0.375</u>	<b>0.374</b>	0.377	0.7
	MAE	0.394	0.390	<u>0.387</u>	<b>0.386</b>	<b>0.386</b>	
ETTh2	MSE	<u>0.287</u>	<b>0.235</b>	0.290	0.290	0.288	0.3
	MAE	<u>0.333</u>	<b>0.301</b>	0.336	0.336	<u>0.333</u>	
ETTm1	MSE	0.316	<b>0.307</b>	0.312	<u>0.309</u>	0.313	0.3
	MAE	0.343	0.345	<u>0.341</u>	<b>0.338</b>	<b>0.338</b>	
ETTm2	MSE	0.173	<b>0.164</b>	0.172	<u>0.171</u>	0.172	0.3
	MAE	0.253	<b>0.247</b>	0.251	<u>0.250</u>	0.251	